CHALMERS

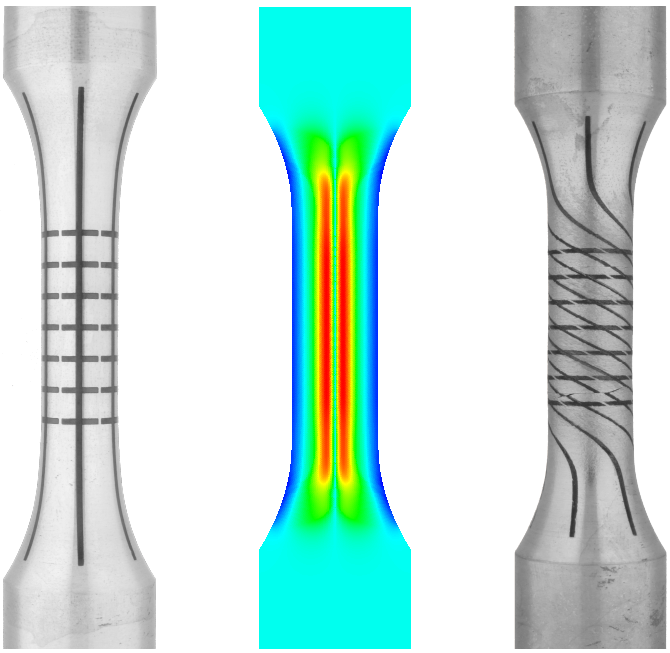

Modeling and experimental characterization of pearlitic rail steels subjected to large biaxial strains

KNUT ANDREAS MEYER

Department of Industrial and Materials Science
CHALMERS UNIVERSITY OF TECHNOLOGY
Göteborg, Sweden 2017

THESIS FOR THE DEGREE OF LICENTIATE OF ENGINEERING IN SOLID AND STRUCTURAL MECHANICS

Modeling and experimental characterization of pearlitic rail steels subjected to large biaxial strains

KNUT ANDREAS MEYER

Department of Industrial and Materials Science
Division of Material and Computational Mechanics
CHALMERS UNIVERSITY OF TECHNOLOGY

Göteborg, Sweden 2017

Modeling and experimental characterization of pearlitic rail steels subjected to large biaxial strains
KNUT ANDREAS MEYER

Thesis for the degree of Licentiate of Engineering IMS-2017-04
Department of Industrial and Materials Science
Division of Material and Computational Mechanics
Chalmers University of Technology
SE-412 96 Göteborg
Sweden
Telephone: +46 (0)31-772 1000

Cover:
Undeformed test bar (left), simulated residual shear stress in a cross-section of the bar (center) and deformed test bar (right).

Chalmers Reproservice
Göteborg, Sweden 2017

Modeling and experimental characterization of pearlitic rail steels subjected to large biaxial strains
Thesis for the degree of Licentiate of Engineering in Solid and Structural Mechanics
KNUT ANDREAS MEYER
Department of Industrial and Materials Science
Division of Material and Computational Mechanics
Chalmers University of Technology

Abstract

Large shear strains develop in the near-surface region under the running band of railway rails. Rolling Contact Fatigue (RCF) cracks often initiate in this region, causing major problems for the railway industry. However, characterization of the constitutive and fatigue behavior of this region is difficult due to the large gradient of properties. In the present thesis, the deformed microstructure in this region is characterized. An axial-torsion test rig is used to predeform cylindrical low-cycle fatigue specimens in order to obtain material properties similar to those of the near-surface region in rails. These specimens are more suitable for further mechanical testing, compared to those resulting from many of the other predeformation methods described in the literature. The obtained material is compared to field samples in terms of the material hardness and microstructure. The microstructure is evaluated with both optical microscopy and scanning electron microscopy. This comparison shows that the predeformed material state closely resembles what is found in some used rails at a depth between 50 and 100 µm.

In order to describe the behavior of the material during the large shear deformations, a sound framework for finite strain metal plasticity is needed. Several options are available in the literature, but in this thesis two frameworks for hyperelasto-plasticity with kinematic hardening are investigated. It is shown that for appropriate choices of Helmholtz' free energy these frameworks are equivalent.

Furthermore, several material models formulated within this framework are evaluated in terms of their abilities to predict the mechanical response during the predeformation. Particular emphasis is put on the role of the kinematic hardening laws and how these influence the response during the biaxial loading. It is found that by combining different models from the literature, the predeformation process can be modeled accurately.

Keywords: Pearlitic steel, hyperelasto-plasticity, biaxial loading, axial-torsion, kinematic hardening

Preface

The work in this thesis was carried out at the Department of Industrial and Materials Science at Chalmers University of Technology from May 2015 to August 2017 within the research project MU34 "Influence of anisotropy on the deterioration of rail materials". This project has been part of the research activities in the National Centre of Excellence CHAlmers Railway MEChanics (CHARMEC). The research has been funded by Chalmers, Trafikverket (via the European Horizon 2020 Joint Technology Initiative Shift2Rail through contract no. 730841), voestalpine Schienen GmbH and the other industrial partners to CHARMEC.

Acknowledgements

I would like to start by thanking my science teachers in chronological order. In Norway, Harald Ruud for letting me explore the sciences (and almost blow up the chemistry lab) and Ivar Helgesen †, Arnt Frode Stava and Anne-Elisabeth Indrebø Haga for challenging me and still trusting me after "warnings" from Harald. Moving forward to Chalmers, I would like to express my gratitude towards Professor Mikael Enelund and the team around him for creating the best mechanical engineering program in Sweden, from which I had the honor of graduating. Last of my teachers, but certainly not the least, my supervisors Professor Magnus Ekh and Professor Johan Ahlström are greatly appreciated for their patience, support and guidance throughout these past two years. The amount of knowledge you possess is only matched by your abilities to share it.

Furthermore, I would like to thank my other co-author Dimitris Nikas for a very interesting and fun cooperation. Håkan Millqvist has been very welcoming and helpful in the materials workshop, for which I am very grateful. My dear friends and colleagues at the divisions of "Materials and Computational Mechanics", "Dynamics" and "Engineering Materials" are also much appreciated, and I'm really glad for all of our interesting discussions about coding, life and anything in-between.

Finally, I would like to thank my family and friends for always being there for me. Especially, I want to thank my parents for the many good values in life and their unconditional love and support. I would not be the man I am today without you.

Thesis

This thesis consists of an extended summary and the following appended papers:

Paper A Meyer, K.A., Nikas, D., Ahlström, J. "Comparison between biaxially deformed pearlitic rail steel and field samples" *Submitted for international publication* (2017)

Paper B Meyer, K.A., Ekh, M. "A comparison of two frameworks for kinematic hardening in hyperelasto-plasticity" *XIV International Conference on Computational Plasticity (COMPLAS 2017)* (2017)

Paper C Meyer, K.A., Ekh, M., Ahlström, J. "Modeling of kinematic hardening at large biaxial deformations in pearlitic rail steel" *Submitted for international publication* (2017)

The appended papers were prepared in collaboration with the co-authors. **Paper A** was a joint work between CHARMEC projects MU28 (Dimitrios Nikas) and MU34, in which the experimental work was shared. In **Paper B** and **Paper C** the author of this thesis was responsible for the major progress of the work, i.e. planning the papers, took part in developing the theory, planning and conducting the experiments, developing the numerical implementations and running the simulations.

Contents

Part I
Extended Summary

1 Introduction

1.1 Background and motivation

A major advantage with railway transportation is the low rolling resistance in the wheel rail contact. Unfortunately this comes at the cost of a very high contact pressure, which can exceed 1000 MPa (Johnson 1989; Pau et al. 2002; Marshall et al. 2006; Wiest et al. 2008). The small contact patch also results in large shear stresses due to the traction and cornering, resulting in wear and severe plastic deformations. These processes lead to large geometric changes of the rail head during service, which are visualized in Figure 1.1a using a field sample from **Paper A**. The severe plastic deformations close to the surface can be seen in the material after etching, through the so-called flow lines visible in Figure 1.1b

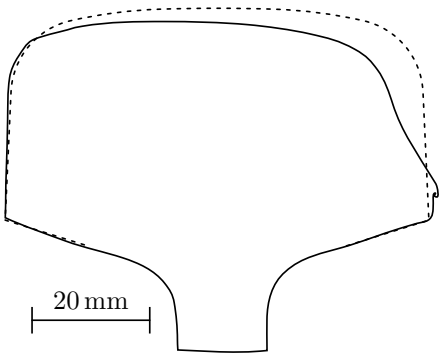

(a) Nominal rail profile (BV50) (dashed) and a worn profile from **Paper A**.

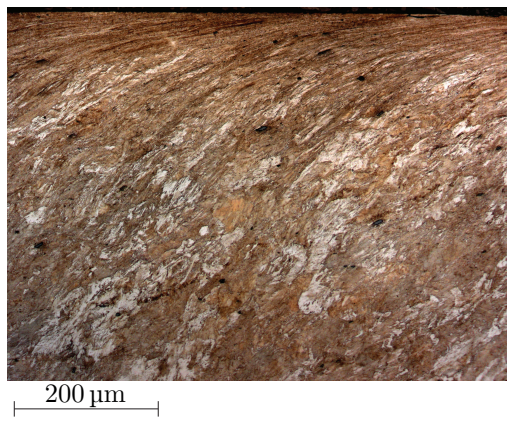

(b) Flow lines showing the highly deformed material at the gauge corner of the rail (45° to longitudinal direction.

Figure 1.1: Visualization of the large deformations in a rail from the Swedish main line between Gothenburg and Stockholm.

It is well known that these large plastic deformations are closely related to the initiation of Rolling Contact Fatigue (RCF) (see Johnson 1989, for an overview). In 2012, the annual cost for railway infrastructure maintenance and renewal across Europe was estimated to be between 15 and 25 billion Euros (EIM-EFRTC-CER WORKING GROUP 2012). The cost of rail defects alone was estimated to 2 billion Euros a year in 2011 by Magel (2011). This equates to an average cost of about 6.7 kEuros per kilometer in Europe's 300 000 km

long railway network (Lidén and Joborn 2016). These costs do not include the lost profit due to scheduled maintenance, nor the loss of profit for business passengers during delays due to unscheduled repairs.

There has been much focus on modeling the large deformations occurring in railway applications within CHARMEC. In particular the projects MU14 (Johansson 2006) and MU19 (Larijani 2014) have addressed the modeling of large plastic deformations. Improved models can both enhance the possibilities of predicting when maintenance is required and give a better understanding of what factors that influence the deterioration processes. This thesis is an intermediate result of the CHARMEC project MU34: "Influence of anisotropy on deterioration of rail materials". The goal of this project is to build upon the previous efforts in MU14 and MU19, with the goal of closing the gap between the modeling and the experimental quantification of rail material behavior under large deformations.

1.2 Aim and scope

The main focus of this thesis is the predeformation of cylindrical rail steel test bars. Such bars can be used to characterize the material behavior close to the surface of the rails, from where rolling contact fatigue cracks often originate. The aims for this thesis are as follows

- Develop a methodology for obtaining test material with similar properties to those of the surface layer in highly deformed rails: The methodology is developed in **Paper C** and verified in **Paper A**.
- Determine an appropriate framework for modeling large elastoplastic cyclic deformations (**Paper B**).
- Investigate the role of kinematic hardening in such frameworks and evaluate appropriate kinematic hardening laws for the modeling of the predeformation (**Paper C**).

The number of techniques that could be used to compare the material state of the obtained test material with field samples of rails is virtually unlimited. In this thesis three different techniques (see Section 2) are considered sufficient to compare field samples with the predeformed material. The material behavior during the predeformation can be modeled by a number of different frameworks. In this thesis we have chosen to consider only phenomenological hyperelasto-plastic models. Further reasoning for this choice is given in Section 3.

2 Experimental techniques

In this chapter many of the experimental techniques used in this thesis are described and discussed. A main focus of this thesis is biaxial axial-torsion testing. It is used to obtain large deformations in low cycle fatigue test bars. The magnitude of the deformations are similar to what is found in the surface-near region of railway rails. Furthermore, the methods that are used to compare microstructures of the predeformed material and the material in the surface layer of rails in **Paper A** are also discussed.

2.1 Biaxial testing

Due to its simplicity, uniaxial testing is a very common method in material testing. However, several authors (e.g. Hassan et al. 1992; Portier et al. 2000; Bari and Hassan 2002; Chen et al. 2005; Abdel-Karim 2009) have shown that the ratcheting behavior of metals cannot be determined with only uniaxial testing. The extension to biaxial (axial-torsion) loading enables a more complete description of the material behavior under complex loading conditions, similar to the loading occurring in the wheel-rail interaction. Several authors have therefore tested rail materials under torsion-compression loading (e.g. Bower 1989; McDowell 1995; Pun et al. 2014), but the strains in those studies are typically much lower than those observed in used rails (cf. Figure 1.1b).

The primary focus of this thesis is predeformation of cylindrical test bars through twisting under different axial loads (see Figure 2.1). The amount of twist to failure is strongly influenced by the nominal axial stress. After a predeformation with a nominal axial load of $-500\,\text{MPa}$, large deformations are visualized by the lines on the test bar in Figure 2.2. The biaxial extensometer that was used is unable to measure such large

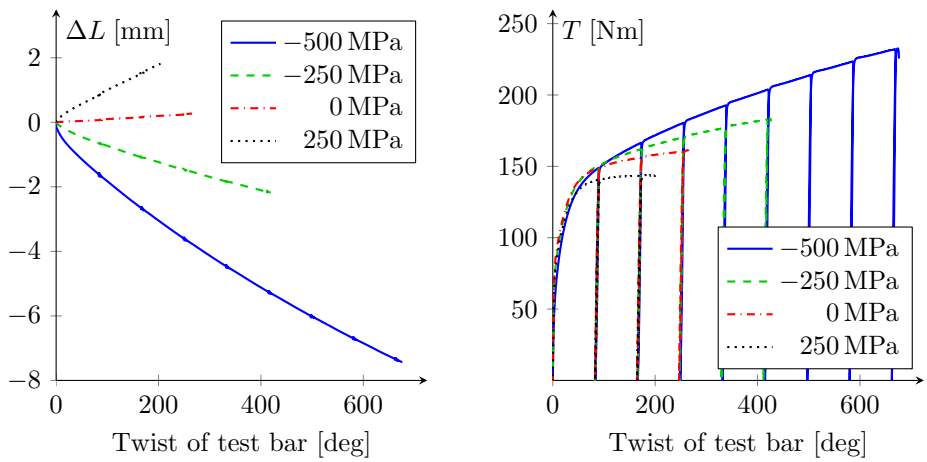

(a) Change of test bar length.

(b) Torque response.

Figure 2.1: Test results at different nominal axial stresses.

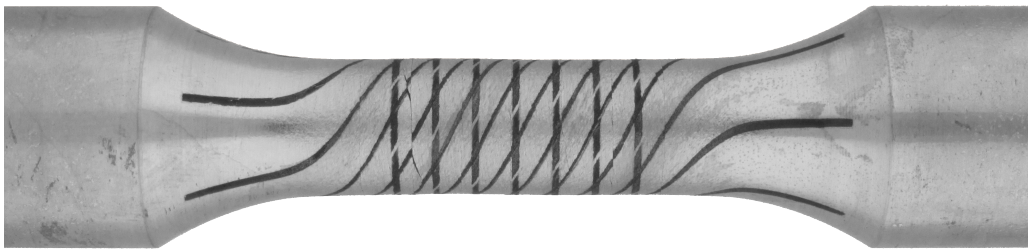

Figure 2.2: Predeformed test bar. The helical lines were initially along the axial direction (i.e. perpendicular to the circumferential lines).

deformations. Hence, the piston position sensors of the machine are used to measure the twist angle and axial displacements presented in Figure 2.1. A method for compensating for the machine stiffness and other effects is described in **Paper C**. To connect the experimental results with the material's constitutive behavior, an axisymmetric finite element model is used in **Paper C**.

In an attempt to measure the local strains some test bars were marked using a grid made by laser engraving. The idea was that the angles between the lines could be used to measure shear strain, and the change of line spacing could be used to measure axial strain. The effect on the failure strain was negligible for a nominal axial compressive load of 500 MPa. However, at zero or tensile axial load the markings strongly influenced the fractures. It was found that martensite formed at the shallow markings, probably causing crack initiation. Even at higher compressive stresses the fracture initiated at the markings, even though this did not influence the amount of twist the bars could sustain before failure. Since the strain fields were not homogeneous around the markings, the marking was not used to measure the surface strains. The overall load versus displacement behavior prior to failure was unaffected by these markings. Apart from the results from the bar with 600 MPa nominal axial load in **Paper C**, no results from bars with laser engraving were used in the appended papers.

A new method for laser marking became available after the testing was completed. This method does not engrave, but burns pigment onto the material surface. Using this method the test bar in Figure 2.2 was predeformed. However, it has not been fully verified yet that this method does not influence the results, but the initial results are promising.

2.2 Hardness testing

Hardness testing allows evaluation of the material's resistance to plastic deformation in very small regions. It can be used to study the hardness difference between various phases in the material or to evaluate the variation of this resistance over an area. In this thesis the pyramid shaped hardness indenters Vickers and Knoop are used. An advantage with the double symmetric Vickers indenter is that the quality of the indent can be evaluated as the ratio between the two nominally equal diagonals that are produced. To avoid measurement influence from neighboring indents there should be sufficient space to other

indents and free surfaces, typically 2.5 times the diagonal (ASTM E92-17 2017). The Knoop indenter produces a 7 to 1 ratio of the indent diagonals, and only the largest diagonal is measured. This allows for closer spaced indents and to measure the hardness closer to the rail surface. The latter is of particular interest in **Paper A**. Furthermore, the more narrow indents gives a higher spatial resolution of the variation with depth. For these reasons the Knoop hardness is used for quantifying the hardness variations with depth, while the Vickers hardness is used to evaluate the hardness where the gradients are smaller.

There exists conversions between the different hardness scales (ASTM E140-12be1 2012). However, the well-known Indentation Size Effect (ISE) (Hays and Kendall 1973) implies that there is a material dependence when converting between different loads (and hence also hardness indenter types) at low loads (ASTM E92-17 2017). To avoid these issues, the comparisons between different samples are conducted using the same hardness method. In addition to the ISE, the very small load (10 g) that was used for the Knoop test in **Paper A** puts high demands on the optical resolution for measuring the indent accurately. This is investigated by comparing with Scanning Electron Microscope (SEM) images of the indents in **Paper A**. It is found that there is a consistent error. This implies that comparative investigations, using the optical measurement system, can be conducted. The accuracies of the absolute hardness values are, however, limited.

A final concern when using hardness measures in a highly deformed structure is that the material properties may be anisotropic. The hardness test is used as a simple measure of the local resistance to plastic flow and it would therefore be favorable if there is no need for samples in multiple directions. Garfinkle and Garlick 1968 found that for BCC and FCC single crystals, the measurement plane had negligible effect on the hardness values

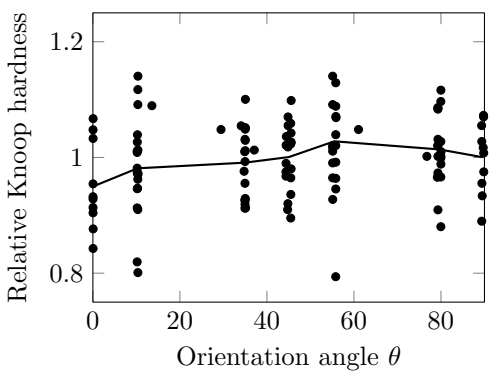

(a) Normalized Knoop hardness (10 g load) variation with major diagonal orientation angle relative to the radial direction.

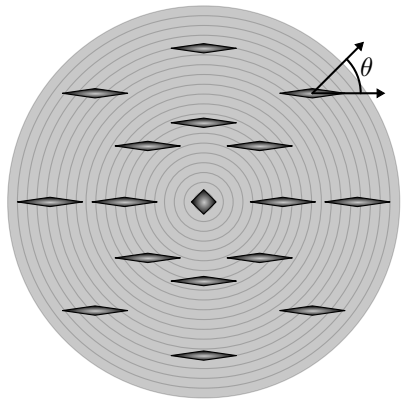

(b) Magnified Knoop indents on a predeformed test bar. The circular lines indicate the axi-symmetric material properties. A Vickers indent with the same area is given as reference in the center.

Figure 2.3: Knoop hardness on predeformed test bars.

when using the Knoop indenter. The direction of the major diagonal of the Knoop indenter did, however, influence the hardness values. This influence was also found by Takeda 1973 for the Vickers indenter in an iron (BCC) crystal. To investigate if such effects influence the measurements in **Paper A**, the Knoop hardness of a predeformed test bar is analyzed in Figure 2.3. Here, the hardness is measured on a plane with the normal in the axial direction of the bar (see **Paper A** for further details on the extraction of the samples). Measurements are taken at different radii and with the major diagonal at different angles relative to the radial direction. The hardness measurements are normalized with the average hardness at the particular radius, to isolate the dependence of the orientation. In comparison to the scatter for each angle, no significant influence from the orientation angle can be identified. We therefore conclude that for the investigated sample, the Knoop hardness can be considered as an isotropic measure of the materials resistance to plastic flow. The same conclusion can also be drawn regarding the Vickers measurements.

2.3 Microstructural quantifications

Pearlitic steel is a composite material structure consisting of hard cementite lamellae embedded in a softer ferrite matrix. The railway rail steel studied in this thesis is the fully pearlitic grade R260. Fully pearlitic indicates that the carbon content is close to the eutectic composition and most of the material is therefore pearlite (the remaining is typically either pure ferrite or grain boundary cementite). The hard cementite lamellae enhance the wear strength of the material, while the softer ferrite contributes to the ductility required to limit crack growth.

Crystalline plastic materials exhibit so called "flow lines" after large amount of shear deformation (see Figure 1.1b). This is commonly observed after e.g. metal cutting operations, but can also be found close to the surface after rolling contact with tangential forces such as in railway applications. This has been used by some authors (cf. Alwahdi et al. 2013; Cvetkovski and Ahlström 2013; Tyfour et al. 1996) to quantify the amount of accumulated shear strain that the material close to the rolling contact surface has experienced. In **Paper A** this is used as a comparison between field samples and predeformed test bars to examine if the same amount of accumulated shear strains is obtained. One complication when using this method is that the lines are obscured by different microstructural elements, leading to difficulties when using softwares for image analysis. A manual approach of tracing the lines on a transparent sheet is therefore adopted in **Paper A**. These sheets are then scanned, and the drawn lines are analyzed using image processing to obtain the tangent lines at different depths. To reduce the operator influence on the line tracing, two different persons trace the same images and the results are averaged. The variation between the operators is typically similar to the variations within each image in terms of the measured angles, although the depth to which the lines are observed differs.

To further understand how the material has been strained, a method using the two dimensional orientation distributions of the cementite lamellae is proposed and used in **Paper A**. A major advantage with this method is that it is operator independent, as the measurements are conducted using an automated image analysis algorithm. This

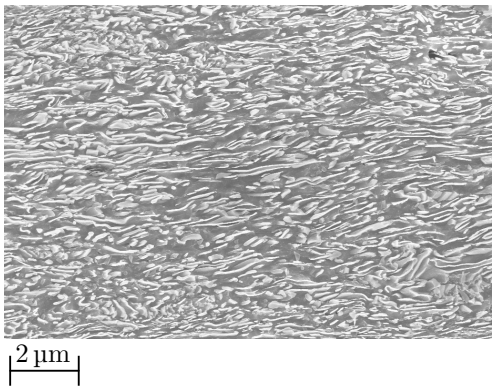

(a) Highly deformed pearlite close to the surface.

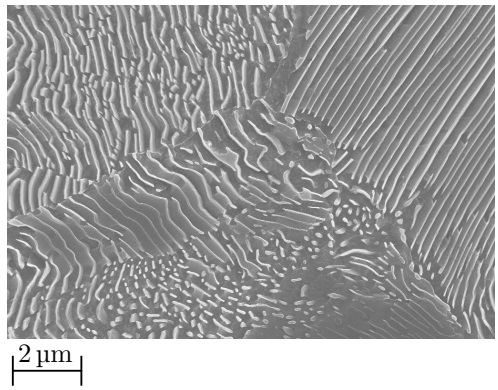

(b) Less deformed pearlite deeper into the rail material.

Figure 2.4: SEM images of the pearlitic microstructur that is used to obtain the lamella orientation distributions in **Paper A**.

is possible since there are fewer disturbing features in the SEM images of the lamellae than in the optical images of the flow lines. A method based on the gradient of the pixel intensity is used to obtain the orientation distributions. The main purpose is to compare the distributions for equivalent acquisition between the field rail samples and the predeformed test bars. Figure 2.4 shows two examples of images used for this study.

Another possible microstructural quantification of the pearlite structure, often used in the literature, is the lamellae spacing. But the large deformation that the material sustains causes breakup, bending and shearing of the lamellae (see Figure 2.4a). The lamellae spacing is therefore not well defined. Furthermore, a reason for the interest in lamellae spacing is the connection to the well-known Hall Petch effect, which states that the hardness increase with decreasing spacing between obstacles for dislocation movement. As the cementite lamellae start deforming plastically, other strengthening mechanisms are becoming more influential (Zhang et al. 2011). The lamellae spacing is then less influential on the material behavior. For these reasons, the lamellae spacing is not considered in **Paper A**.

3 Material modeling

Two main categories of constitutive models for finite element analyzes are found in the literature; phenomenological and multiscale models. For the pearlitic steel used in this thesis, there has been quite some work on multiscale models (e.g. Allain and Bouaziz 2008; Berisha et al. 2015; Laschet et al. 2013; Lindfeldt 2014; Peng et al. 2002; Terada et al. 2004). But large strain plasticity is still most commonly simulated with phenomenological models (e.g. Dettmer and Reese 2004; Grilo et al. 2016; Johansson et al. 2005; Johansson et al. 2006; Menzel et al. 2005; Vladimirov et al. 2008; Wallin et al. 2003; Wallin and Ristinmaa 2005), which are more or less motivated by the underlying mechanisms and microstructures. Larijani et al. 2013 proposed a hybrid model, obtaining a relatively fast model while still incorporating some microstructural features through an analytical homogenization (involving a numerical integration). The work in this thesis should be applicable for simulating repeated rolling contact loads with a reasonable computational time. The modeling is therefore limited to phenomenological models.

3.1 Modeling framework

Finite element models often assume small deformations, which results in computational efficient simulations. However, in some applications, such as in sheet metal forming and in the wheel-rail rolling contact, it is necessary to account for the large deformations. In the literature, there are two model types that account for large deformations: Hypo-models and hyper-models. Hypo-models typically extend the small strain formulations using different objective stress rates. These models are common in commercial finite element softwares. In Abaqus (Abaqus 2013) the co-rotational formulation approximated according to Hughes and Winget 1980 is used. An advantage with this formulation is that small strain model implementations can conveniently be used when accounting for large deformations. When using von Mises plasticity with linear kinematic hardening (a special case of the Chaboche model, cf. Chaboche 1986) for simulating simple shear of a $1 \times 1 \times 1\,\text{mm}$ box, the result in Figure 3.1a is obtained. This load case with large shear deformation is similar to the deformation seen at the top of the rail in Figure 1.1b. The simulation shows a non-physical oscillatory response in the reaction force, motivating the need for adopting another modeling framework. There exists hypo-models in literature not showing this behavior (cf. Grilo et al. 2016), but in this thesis hyper-models are adopted. The main motivation for adopting hyper-models is that they are inherently thermodynamically consistent (i.e. they fulfill the second law of thermodynamics).

Two frameworks of hyperelasto-plastic models with kinematic hardening are considered in this thesis: The first was suggested by Wallin et al. 2003 and the second by Dettmer and Reese 2004. These frameworks are compared in **Paper B** where it is shown that for the same choice of free energy they coincide.

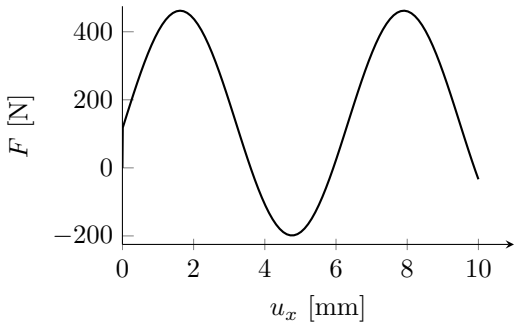

(a) Force versus displacement.

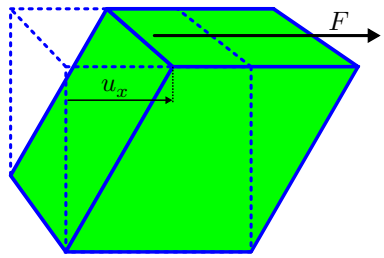

(b) Simple shear of a $1 \times 1 \times 1$ mm box.

Figure 3.1: Simulation of simple shear in Abaqus using von Mises plasticity and linear kinematic hardening.

3.2 Kinematic evolution laws

In **Paper C** particular emphasis is put on the kinematic evolution laws, and a brief discussion on various suggestions found in the literature is therefore given here. The different evolution laws are adapted to the large strain frameworks in **Paper C**, and compared to the mechanical response during the predeformation of the test bars. For further details on the notation the reader is referred to **Paper C**.

A commonly used kinematic hardening law in metal plasticity is the Armstrong-Frederick (AF) model. It combines the original Linear Kinematic Hardening (LKH) law, suggested by Prager 1955, with the Dynamic Recovery (DR) term, suggested by Armstrong and Frederick in 1966 (Frederick and Armstrong 2007). Although quite efficient at capturing cyclic plastic behavior, it often overpredicts ratcheting (cf. Abdel-Karim 2009; Bari and Hassan 2002; Chen et al. 2005; Delobelle et al. 1995; Portier et al. 2000). An alternative evolution law was proposed by Ohno and Wang 1993 (denoted the Ohno-Wang (OW) model), which improves the ratcheting prediction in some cases. But Bari and Hassan 2002 showed that neither of these laws are accurate at predicting the ratcheting for non-proportional biaxial loading. The suggestion by Delobelle et al. 1995 to combine the AF rule with the Radial Evanescence (RE) term proposed by Burlet and Cailletaud 1986 is shown in Equation (3.1):

$$\boldsymbol{\nu}_{\mathrm{k},i}^{\mathrm{BC}} = \underbrace{-\boldsymbol{\nu}}_{\mathrm{LKH}} + \delta \underbrace{\frac{3}{2}\frac{\boldsymbol{M}_{\mathrm{k},i}^{\mathrm{t}}}{Y_{\mathrm{k},i}}}_{\mathrm{DR}} + (1-\delta) \underbrace{\left(\frac{\boldsymbol{M}_{\mathrm{k},i} : \boldsymbol{\nu}}{Y_{\mathrm{k},i}}\right)\boldsymbol{\nu}}_{\mathrm{RE}} \tag{3.1}$$

By using this suggestion it was found in Johansson et al. (2005) that very good predictions of multiaxial ratcheting experiments could be obtained. Burlet and Cailletaud's radial evanescence term has also been combined with the OW model (Chen et al. 2005), also yielding good predictions for similar experiments. Other combinations of these two models are also possible, as demonstrated by Abdel-Karim 2009.

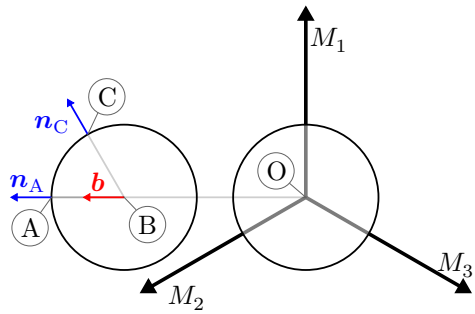

Figure 3.2: Illustration of the translation of the yield surface due to kinematic hardening during the loading path O-A-B-C. The principal stress directions are fixed, and the view is along the hydrostatic axis ($M_1 = M_2 = M_3$) with a von Mises yield surface.

The main difference between the AF/OW models and the radial evanescence term is the direction of the saturation, which is illustrated in Figure 3.2. While the AF/OW models' saturation terms are both along the direction of the current back-stress $\boldsymbol{b} = \boldsymbol{M}^{\mathrm{t}}_{\mathrm{k},i} / \left|\left|\boldsymbol{M}^{\mathrm{t}}_{\mathrm{k},i}\right|\right|$, the radial evanescence term is directed along the current yield surface normal $\boldsymbol{n} = \boldsymbol{\nu} / ||\boldsymbol{\nu}||$. For the proportional loading path O-A these directions coincide. For a small strain formulation the parameter δ has no influence for proportional loading, but this is not exactly fulfilled for a large strain formulation. Let us consider the unloading to the center of the yield surface (A-B) and then loading along the B-C direction. This type of non-proportional loading results in different directions of the back-stress $\boldsymbol{b}$ and the yield surface normal $\boldsymbol{n}$. The radial evanescence term is along $\boldsymbol{n}$, scaled with the scalar projection of the dynamic recovery term onto $\boldsymbol{n}$. By combining these two evolution laws an additional model choice of the direction of back-stress evolution for non-proportional loading is obtained. This seems to greatly improve the ability to predict the multiaxial ratcheting. It was shown by Bari and Hassan 2002 that it suffices to introduce a single material parameter δ (irrespective of the number of back-stresses) to obtain an accurate model.

In **Paper C** it is shown that this type of model can also be used to simulate the large torsion-compression predeformation of the test bars. Some fitted results are shown in Figure 3.3. The predicted results for different axial loads in **Paper C** are also very accurate in terms of the overall response. However, the detailed loop shape is neither captured for the fitted response, nor for the predicted response in Figure 3.4.

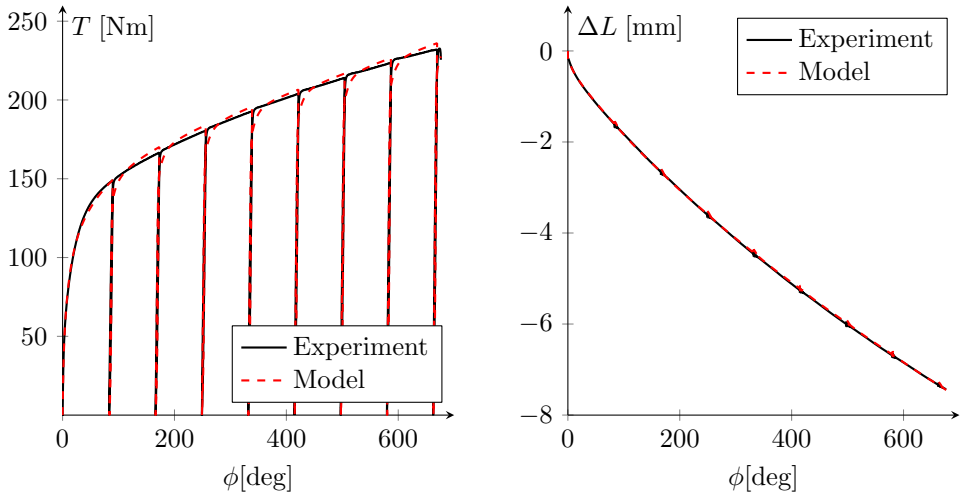

(a) Torque.

(b) Axial displacement.

Figure 3.3: Fitted results to a predeformation experiment with a nominal axial load of −500 MPa, using the evolution law in Equation (3.1).

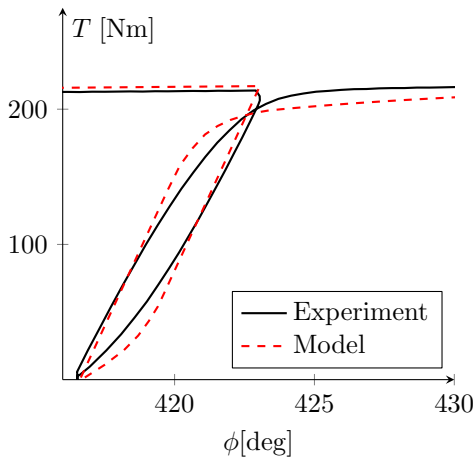

Figure 3.4: Prediction of loop shape for an experiment with a nominal axial load of −600 MPa, using the evolution law in Equation (3.1)

4 Summary of appended papers

Paper A: **Comparison between biaxially deformed pearlitic rail steel and field samples**

In this paper we evaluate if the predeformation method is able to produce test material representative of the material found at the top of the rail head. The materials are evaluated in terms of hardness, accumulated shear strain and microstructural reorientation. In addition to the very consistent mechanical response during the predeformation, it is found that the predeformed test bars are very consistent in terms of these three evaluation methods. The obtained test material is also found to be quite representative of rail material, which seems to have experienced unidirectional loading, at a depth of 50 to 100 µm. As the material fails during the predeformation, it is not possible to represent the material behavior closer to the rail surface. However, this paper shows that the samples produced by twisting the cylindrical test bars can be used to characterize the material behavior close to the rolling surface of rails.

Paper B: **A comparison of two frameworks for kinematic hardening in hyperelasto-plasticity**

It is shown that the two considered frameworks for kinematic hardening in hyperelasto-plasticity (from Wallin et al. 2003 and Dettmer and Reese 2004) are equivalent, provided that the same formulations for free energy is used. The equivalence is shown both analytically and numerically. A model within this framework is tested with very large simple shear deformations (up to $F_{12} = 50$) and does not exhibit any oscillations. The flexibility in extending this framework to anisotropy and potentially also damage, motivates the choice of using it for coming studies.

Paper C: **Modeling of kinematic hardening at large biaxial deformations in pearlitic rail steel**

The main focus of this paper is to evaluate different kinematic evolution laws in the framework described in **Paper B**. The material models are evaluated using an axi-symmetric finite element simulation of the predeformation experiments. A material parameter identification procedure is used to identify the optimal parameter values for predeformation with a nominal axial load of -500 MPa, and the predictive abilities are investigated for two other load cases. It is found that the combination of the radial evanescence term from Burlet and Cailletaud 1986, with either the Armstrong-Frederick (Frederick and Armstrong 2007) or the Ohno-Wang (Ohno and Wang 1993) saturation terms, gives an accurate model for the material behavior. A method for compensating for errors in the axial torsion test rig used for the predeformation experiments is also discussed in an appendix.

5 Future work

The characterization of the predeformed test bars in **Paper A** shows that the predeformation is method can be used to obtain a deformed material that is similar to what is found in used rails. However, the deformed bars have gradients of their properties along the radius. Additionally, during twisting of (long) solid bars the shear strain varies linearly with the radius causing a non-homogeneous stress field. These effects imply that a finite element solution is necessary to couple test results with the constitutive behavior. By drilling out the deformed bars, thin-walled test bars, which are illustrated in Figure 5.1, can be obtained. These have a test volume with a fairly homogeneous material and strain, alleviating the need for a finite element model. Such bars will therefore be tested to understand how the large shear deformation influences the low-cycle fatigue behavior.

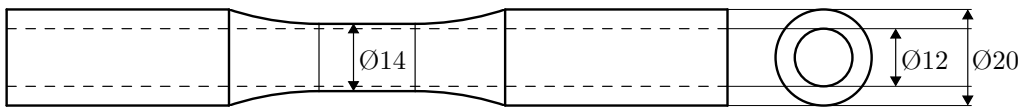

Figure 5.1: Planned thin walled test bars (dimensions in mm).

As mentioned in **Paper C** it is likely that the yield surface is distorted due to the large deformations. It is therefore of interest to characterize the yield surface's shape and location after the predeformation. Further ratcheting experiments will also be conducted to determine cyclic plasticity models for this, presumed, anisotropic material. For these experiments, both proportional and non-proportional loading should be considered.

It is also of interest to obtain information on fatigue life when taking the anisotropy into account. The fatigue life for different loading directions after the predeformation will therefore be compared. The final aim of the project MU34 is to use the models to predict the plastic deformations and fatigue during the rolling contact conditions encountered in railway applications.

References

Abaqus (2013). *Abaqus Theory Guide*. 6.13. Providence, RI, USA: Dassault Systèmes.

Abdel-Karim, M. (2009). Modified kinematic hardening rules for simulations of ratchetting. *International Journal of Plasticity* **25**.8, 1560–1587.

Allain, S. and Bouaziz, O. (2008). Microstructure based modeling for the mechanical behavior of ferrite-pearlite steels suitable to capture isotropic and kinematic hardening. *Materials Science and Engineering A* **496**.1-2, 329–336.

Alwahdi, F. A. M., Kapoor, A., and Franklin, F. J. (2013). Subsurface microstructural analysis and mechanical properties of pearlitic rail steels in service. *Wear* **302**.1-2, 1453–1460.

ASTM E140-12be1 (2012). *Standard Hardness Conversion Tables for Metals Relationship Among Brinell Hardness, Vickers Hardness, Rockwell Hardness, Superficial Hardness, Knoop Hardness, Scleroscope Hardness, and Leeb Hardness*. West Conshohocken, PA.

ASTM E92-17 (2017). *Standard Test Methods for Vickers Hardness and Knoop Hardness of Metallic Materials*. West Conshohocken, PA.

Bari, S. and Hassan, T. (2002). An advancement in cyclic plasticity modeling for multiaxial ratcheting simulation. *International Journal of Plasticity* **18**.7, 873–894.

Berisha, B. et al. (2015). Multiscale modeling of failure initiation in a ferritic-pearlitic steel. *Acta Materialia* **100**, 191–201.

Bower, A. F. (1989). Cyclic hardening properties of hard-drawn copper and rail steel. *Journal of the Mechanics and Physics of Solids* **37**.4, 455–470.

Burlet, H. and Cailletaud, G. (1986). Numerical techniques for cyclic plasticity at variable temperature. *Engineering Computations* **3**.2, 143–153.

Chaboche, J. (1986). Time-independent constitutive theories for cyclic plasticity. *International Journal of Plasticity* **2**.2, 149–188.

Chen, X., Jiao, R., and Kim, K. S. (2005). On the Ohno-Wang kinematic hardening rules for multiaxial ratcheting modeling of medium carbon steel. *International Journal of Plasticity* **21**.1, 161–184.

Cvetkovski, K. and Ahlström, J. (2013). Characterisation of plastic deformation and thermal softening of the surface layer of railway passenger wheel treads. *Wear* **300**.1-2, 200–204.

Delobelle, P., Robinet, P., and Bocher, L. (1995). Experimental study and phenomenological modelization of ratchet under uniaxial and biaxial loading on an austenitic stainless steel. *International Journal of Plasticity* **11**.4, 295–330.

Dettmer, W. and Reese, S. (2004). On the theoretical and numerical modelling of Armstrong-Frederick kinematic hardening in the finite strain regime. *Computer Methods in Applied Mechanics and Engineering* **193**.1, 87–116.

EIM-EFRTC-CER WORKING GROUP (2012). Track Maintenance & Renewal.

Frederick, C. O. and Armstrong, P. J. (2007). A mathematical representation of the multiaxial Bauschinger effect. *Materials at High Temperatures* **24**.1, 1–26.

Garfinkle, M. and Garlick, R. G. (1968). A stereographic representation of Knoop hardness anisotropy. *Trans. Metall. Soc. AIME* **242**.November, 809–814.

Grilo, T. J. et al. (2016). A finite strain constitutive model for non-quadratic yield criteria and nonlinear kinematic/isotropic hardening: application to sheet metal forming. *Archive of Applied Mechanics* **86**.1, 1–17.

Hassan, T., Corona, E., and Kyriakides, S. (1992). Ratcheting in cyclic plasticity, part II: Multiaxial behavior. *International Journal of Plasticity* **8**.2, 117–146.

Hays, C. and Kendall, E. G. (1973). An analysis of Knoop microhardness. *Metallography* **6**.4, 275–282.

Hughes, T. J. R. and Winget, J. (1980). Finite rotation effects in numerical integration of rate constitutive equations arising in large-deformation analysis. *International Journal for Numerical Methods in Engineering* **15**.12, 1862–1867.

Johansson, G. (2006). "On the modeling of large ratcheting strains and anisotropy in pearlitic steel". PhD thesis. Chalmers University of Technology.

Johansson, G., Ahlström, J., and Ekh, M. (2006). Parameter identification and modeling of large ratcheting strains in carbon steel. *Computers and Structures* **84**.15-16, 1002–1011.

Johansson, G., Ekh, M., and Runesson, K. (2005). Computational modeling of inelastic large ratcheting strains. *International Journal of Plasticity* **21**.5, 955–980.

Johnson, K. (1989). The Strenght of Surfaces in Rolling Contact. *Journal of Mechanical Engineering Science* **203**.December 1988, 151–163.

Larijani, N. (2014). "Anisotropy in pearlitic steel subjected to rolling contact fatigue - modelling and experiments". PhD thesis. Chalmers University of Technology.

Larijani, N., Johansson, G., and Ekh, M. (2013). Hybrid micro-macromechanical modeling of anisotropy evolution in pearlitic steel. *European Journal of Mechanics - A/Solids* **38**, 38–47.

Laschet, G. et al. (2013). Derivation of anisotropic flow curves of ferrite-pearlite pipeline steel via a two-level homogenisation scheme. *Materials Science and Engineering: A* **566**, 143–156.

Lidén, T. and Joborn, M. (2016). Dimensioning windows for railway infrastructure maintenance: Cost efficiency versus traffic impact. *Journal of Rail Transport Planning & Management* **6**.1, 32–47.

Lindfeldt, E. (2014). "On multiscale modeling of pearlitic steel". PhD thesis. Chalmers University of Technology.

Magel, E. E. (2011). *Rolling Contact Fatigue: A Comprehensive Review*. Tech. rep. November. Federal Railroad Administration, p. 118.

Marshall, M. B. et al. (2006). Experimental characterization of wheel-rail contact patch evolution. *Journal of Tribology* **128**.3, 493–504.

McDowell, D. L. (1995). Stress state dependence of cyclic ratchetting behavior of two rail steels. *International Journal of Plasticity* **11**.4, 397–421.

Menzel, A. et al. (2005). A framework for multiplicative elastoplasticity with kinematic hardening coupled to anisotropic damage. *International Journal of Plasticity* **21**.3, 397–434.

Ohno, N. and Wang, J.-D. (1993). Kinematic hardening rules with critical state of dynamic recovery, part I: formulation and basic features for ratchetting behavior. *International Journal of Plasticity* **9**.3, 375–390.

Pau, M., Aymerich, F., and Ginesu, F. (2002). Distribution of contact pressure in wheel–rail contact area. *Wear* **253**.1-2, 265–274.

Peng, X., Fan, J., and Yang, Y. (2002). A microstructure-based description for cyclic plasticity of pearlitic steel with experimental verification. *International Journal of Solids and Structures* **39**.2, 419–434.

Portier, L. et al. (2000). Ratchetting under tension-torsion loadings: experiments and modelling. *International Journal of Plasticity* **16**.3, 303–335.

Prager, W. (1955). The theory of plasticity: A survey of recent achievements. *Proc. Inst. Mech. Engrs* **169**, 41–57.

Pun, C. L. et al. (2014). Ratcheting behaviour of high strength rail steels under bi-axial compression-torsion loadings: Experiment and simulation. *International Journal of Fatigue* **66**, 138–154.

Takeda, T. (1973). The Effects of Temperature and Carbon Content on Vickers Hardness and Its Anisotropy of Iron Single Crystals. *Japanese Journal of Applied Physics* **12**.7, 974–977.

Terada, K. et al. (2004). Numerical re-examination of the micro-scale mechanism of the Bauschinger effect in carbon steels. *Computational Materials Science* **31**.1-2, 67–83.

Tyfour, W., Beynon, J., and Kapoor, A. (1996). Deterioration of rolling contact fatigue life of pearlitic rail steel due to dry-wet rolling-sliding line contact. *Wear* **197**.1-2, 255–265.

Vladimirov, I. N., Pietryga, M. P., and Reese, S. (2008). On the modelling of non-linear kinematic hardening at finite strains with application to springback - Comparison of time integration algorithms. *International Journal for Numerical Methods in Engineering* **75**.1, 1–28.

Wallin, M. and Ristinmaa, M. (2005). Deformation gradient based kinematic hardening model. *International Journal of Plasticity* **21**.10, 2025–2050.

Wallin, M., Ristinmaa, M., and Ottosen, N. S. (2003). Kinematic hardening in large strain plasticity. *European Journal of Mechanics - A/Solids* **22**.3, 341–356.

Wiest, M. et al. (2008). Assessment of methods for calculating contact pressure in wheel-rail/switch contact. *Wear* **265**.9, 1439–1445.

Zhang, X. et al. (2011). Microstructure and strengthening mechanisms in cold-drawn pearlitic steel wire. *Acta Materialia* **59**.9, 3422–3430.